Effect of Zr/Ti ratio on microstructure and electrical properties of pyroelectric ceramics for energy harvesting applications

Qingping Wang[a,b], Jiahui Ma[a] , Chris R. Bowen[c], Mingyu Li[a] , Gong Qiu[a],

Shenglin Jiang[a,*]

[a]*School of Optical and Electronic Information, Huazhong University of Science and Technology, Wuhan 430074, PR China*

[b]*Department of Physics & Mechanical and Electronic Engineering, Hubei University of Education, Wuhan 430205, PR China*

[c]*Materials Research Centre, Department of Mechanical Engineering, University of Bath, Claverton Down Road, Bath BA2 7AY, UK*

Corresponding author: Shenglin Jiang

E-mail: jslhust@gmail.com

Phone and Fax No.: 86-27-87542693

Abstract: In this paper, $Pb[(Mn_xNb_{1-x})_{1/2}(Mn_xSb_{1-x})_{1/2}]_y(Zr_zTi_{1-z})_{1-y}O_3$ (lead magnesium niobate-lead antimony-manganese-lead zirconate titanate: PMnN-PMS-PZT) ceramics with three different Zi/Ti compositions of 95/5 (Zr95), 85/15 (Zr85) and (Zr85+Zr95) were successfully fabricated and characterized. The effect of Zr/Ti ratio on the microstructure and electric properties were studied in detail. The pyroelectric coefficient of Zr95 ceramic was 5957 uC/cm^{2}K which was more than 2 - 3 times higher than other reported pyroelectric ceramics. The effect on pyroelectric energy harvesting was systemically investigated via a variation of Zr/Ti compositions in the ceramics, which was directly evaluated by the output power acquired from the data acquisition system. The output power was 25.7uW, 4.8uW and 14.2uW at a composition ratio of Zr95, Zr85 and Zr85+Zr95, respectively under identical conditions. Among the three Zi/Ti compositions, the best pyroelectric and ferroelectric properties were achieved with Zr95, which indicated that the pyroelectric energy harvesting can be efficiently optimized by the appropriate control of phase

structure.

Key words: Zr/Ti molar ratio, pyroelectric ceramic, electrical properties, energy harvesting

1. Introduction

Energy harvesting is currently a topic of intense interest as a result of the growing energy demands of society and need to power a large number of wireless sensors, as demanded by the Internet of Things (IoTs) [1-3]. Applications of energy harvesters include battery-free portable devices and wireless sensor networks, which can act as a green power with an extended the lifetime compared with the devices with battery. Methods to scavenge energy from ambient environment to generate electrical power have been considered by a number of researchers, one of which is known as the pyroelectric energy harvesting that offers a direct way to convert waste heat into electrical energy by harvesting temperatures fluctuations [6]. Specifically, this approach makes use of the pyroelectric effect to generate a flow of charge to or from the surface of a pyroelectric material as a result of heating or cooling [1]. The short circuit electric current (I) generated by a pyroelectric material during heating and cooling can be defined as

$$I = A \cdot p \cdot (dT / dt) \tag{1}$$

Where p, A and dT / dt are the pyroelectric coefficient, effective electrode area and rate of change in temperature, respectively [1]. Equation (1) shows that the amount of current is determined with a combination of the magnitude of the pyroelectric coefficient p, the size of the electrode area A and on the rate of change in the temperature across the pyroelectric device. Meanwhile, the output power of the pyroelectric device can be expressed as

$$P = U_o^2 / R \tag{2}$$

Where U_o and R are the output voltage and load resistance.

Therefore, in order to improve the output power, researchers are attempting to

increase pyroelectric coefficient of pyroelectric ceramics via a variation of composition and structure as well as experiment conditions. For example, the maximum pyroelectric coefficient of lead strontium titanate (PST) ceramics was obtained under a DC bias 6000 uC/cm^{2}K [7]. Meanwhile, the pyroelectric coefficient reached at 9500 uC/cm^{2}Kby using porous barium strontium titanate (BST) ceramics under DC bias field [8]. Using a melt-blending method, an organosilicate(OS)/poly(vinylidene fluoride)(PVDF) composite has the highest pyroelectric coefficient of 26.7 uC/m^{2}K [9]. Gallagher et al. [10] used a commercial lead indium niobate-lead magnesium niobate-lead titanate (PIN-PMN-PT) single crystal to investigate the pyroelectric coefficient by an applied voltage experiment, and the maximum value reached 650u C/m^{2}K. Recently, lead magnesium niobate-lead titanate (PMN-PT) ceramics has been synthesized by solid-state reaction technique using colunbite precursor, and a larger value of pyroelectric coefficient with 2739 uC/m^{2}K was obtained [11]. Similarly, the pyroelectric coefficient of PMnN-PMS-PZT pyroelectric ceramics could reach 2650 uC/cm^{2}K [12]. Vaish et al. [13] and Bowen et al. [14] also investigated the pyroelectric properties by using different methods for application in energy harvesting.

It is important to note that large pyroelectric coefficients are desirable for energy harvesting applications since naturally occurring temperature fluctuations are generally slow and hence more attention is needed to propose efficient and technologically viable solutions .The Zr-rich lead zirconate titanate ceramics (PZT) are common pyroelectric ceramics, and there is low temperature rhombohedral (F_{RL})-high temperature rhombohedral (F_{RH}) ferroelectric phase transition, which is far lower than the temperature from ferroelectric to paraelectric phase (Tc). Particularly, there is almost no change of dielectric constant during this phase transition [15].

When the F_{RL}-F_{RH} phase transition is induced by temperature, a nonlinear change of spontaneous polarization occurs. Therefore, a large pyroelectric coefficient is obtained, which can be potentially used for heat to electrical conversion such as pyroelectric energy harvesting and thermal imaging [16]. As mentioned, the output power response can strongly depend on the pyroelectric coefficient, thus, a significant

improvement on power response can be expected with Zr-rich PMnN-PMS-PZT ceramics. However, to our knowledge, there are relatively few reports concerning on the enhanced pyroelectric current obtained from F_{RL}-F_{RH} phase transition of Zr-rich PMnN-PMS-PZT ceramics with different Zi/Ti compositions.

The present study is an attempt to enhance the output voltage of PMnN-PMS-PZT ceramics fabricated by modified solid-state reaction technique by investigating the effects of Zr/Ti ratio on the F_{RL}-F_{RH} phase transition and improve the pyroelectric energy harvesting of PMnN-PMS-PZT ceramics.

2. Experimental procedure

$Pb[(Mn_xNb_{1-x})_{1/2}(Mn_xSb_{1-x})_{1/2}]_y(Zr_zTi_{1-z})_{1-y}O_3$ (PMnN-PMS-PZT) pyroelectric ceramics with varied compositions were prepared by modified solid-state reaction technique, in which PbO (99%), ZrO_2(99.9%), TiO_2 (99.8%), Nb_2O_5(99.5%), Sb_2O_3(99%) were used as the starting raw materials. $Mn(NO_3)$ (50%) and deionized water were used as solvents. A 10 mol% excess of PbO was introduced to compensate for the lead loss during the following high-temperature sintering and to prevent the formation of pyrochlore phase in the ceramics. These precursors were stoichiometrically mixed by ball milling for 4h. Calcination was performed at 700°C for 3h followed by ball milling for 4h. The polycrystalline powder was subsequently uniaxailly pressed at 8 MPa into a disk of 15 mm in diameter using polyvinyl acetate (PVA) as a binder. The compacted pellets were sintered at 1230 °C for 4h in air. Parallel-sided disk specimens with a thickness of 0.3 mm were polished and silver electrodes were screen printed onto both surfaces of the samples and they were fired at 600 °C for 25 min. All the samples were poled under 30 kV/cm dc field at 120 °C for 30 min in silicon oil and aged for 24 h.

The bulk density of the samples were measured by the Archimedes method and the average density was approximately 7.8 g/cm^3. The microstructures of the samples were analyzed by X-ray diffraction (X'Pert-PRO, PANalytical B.V.) and field-emission scanning electron microscopy (FE-SEM Sirion 200, FEI), respectively. The dielectric constant (relative permittivity) and loss tangent as a function of temperature were measured with a precision impedance analyzer (Agilent 4294A;

Agilent Technology Inc., Santa Clara, CA). Polarization versus electric field (P-E) hysteresis loops were obtained at 10 Hz on PMF1011-277. The pyroelectric coefficient was measured with a standard Byer-Roundy method by an in-house pyroelectric parameter tracer.

To study the potential of the materials for pyroelectric energy harvesting, a Peltier cell and temperature controller were set-up to maintain time fluctuations of temperature from room temperature (≈20°C) to 65°C, and a PC-based data acquisition system was used to record the output current and voltage of pyroelectric devices. LabVIEW was used to import data from the data acquisition card (NI-USB6002).

3. Results and Discussion

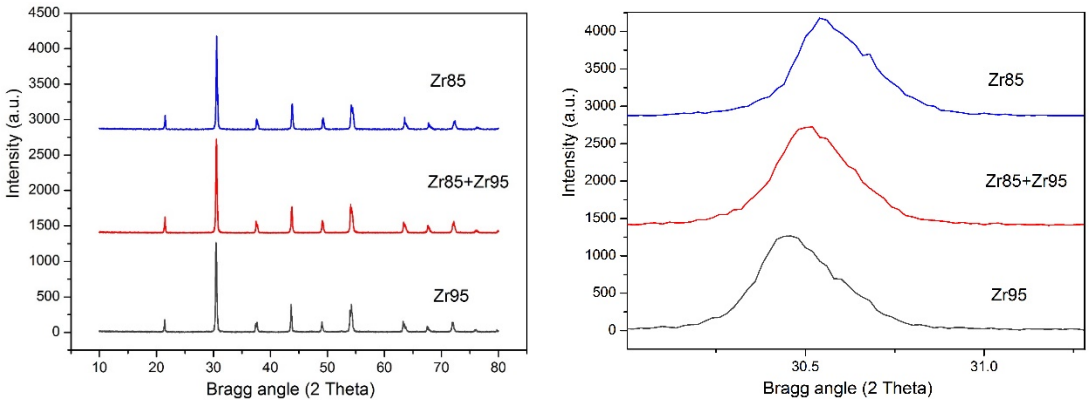

Fig.1. XRD patterns of PMnN-PMS-PZT ceramic at room temperature

Figure 1 shows the XRD patterns of PMnN-PMS-PZT ceramic at room temperature after being annealed at 1230°C, which were recorded with a step size of 0.02° at a scanning rate of 2°/min within 2θ from 10° to 90°。The diffraction peaks were indexed with space group in agreement with the respective Joint Committee on Powder Diffraction Standards (JCPDS) card no 20-0608. The presence of sharp and well-defined peaks indicate that this ceramic has pure perovskite phase with a good degree of crystallinity and no secondary phase formation, such as pyrochlore, was detected. However, the diffraction peaks shift to a lower angle on increasing the Zr content, this is because the larger Zr^{+4} replaces the smaller Ti^{+4} [17], which results in an increase of the unit cell volume.

The lattice constant calculated from the XRD patterns of the ceramics is shown in Table 1. As the Zr content increased from 0.85 to 0.95, the lattice constant α also

increased. The pyroelectric effect is described in terms of a vector, the pyroelectric coefficient p given by the rate of change of the spontaneous polarization (P_s) with the temperature [18], see equation 3, and P_s is related to the crystal structure. The direction of P_s in pyroelectric materials with a perovskite phase appears along the c axis. Thus, a larger length along the c-axis should lead to a larger value of P_s.

$$p = \frac{\partial P_S}{\partial T}_{E\sigma} \tag{3}$$

Table 1 Lattice constant derived from X-ray diffraction patterns of the ceramics with various Zr contents

Sample	α /nm	b /nm	c /nm
Zr85	0.4112	0.4112	0.4006
Zr85+Zr95	0.4111	0.4111	0.4109
Zr95	0.4117	0.4117	0.4123

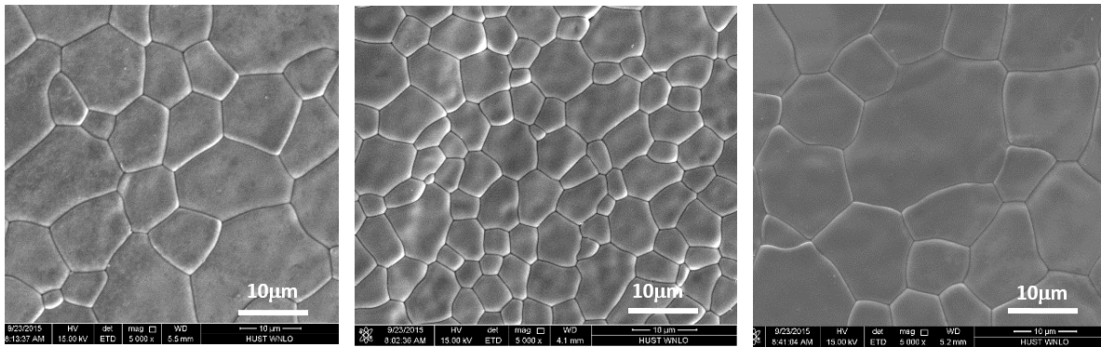

(a) (b) (c)

Fig.2. SEM micrographs of the surface morphology of the ceramics (a) Zr/Ti=85/15 (b) Zr85+Zr95, (c) Zr/Ti=95/5

Figure 2 shows the SEM images of the surfaces of the ceramics. All the ceramics exhibited a dense, fine grained and uniform microstructure. There were no microcracks or other microstructural defects found in all the ceramics. The average grain size was approximately 5, 8 and 15um for the three ceramics Zr95, Zr85 and Zr85+Zr95 shown in Fig.2 (a), (b) and (c) respectively, which was calculated by using the Nano Measurer software. As the Zr content increased, the grain size also gradually

increased. This indicated that the increase of Zr content enhanced the sintering which was beneficial to the crystal growth and density of the ceramics.

The temperature-dependent relative permittivity of the pyroelectric ceramics are shown in Figure 3, which were measured at 1 kHz during

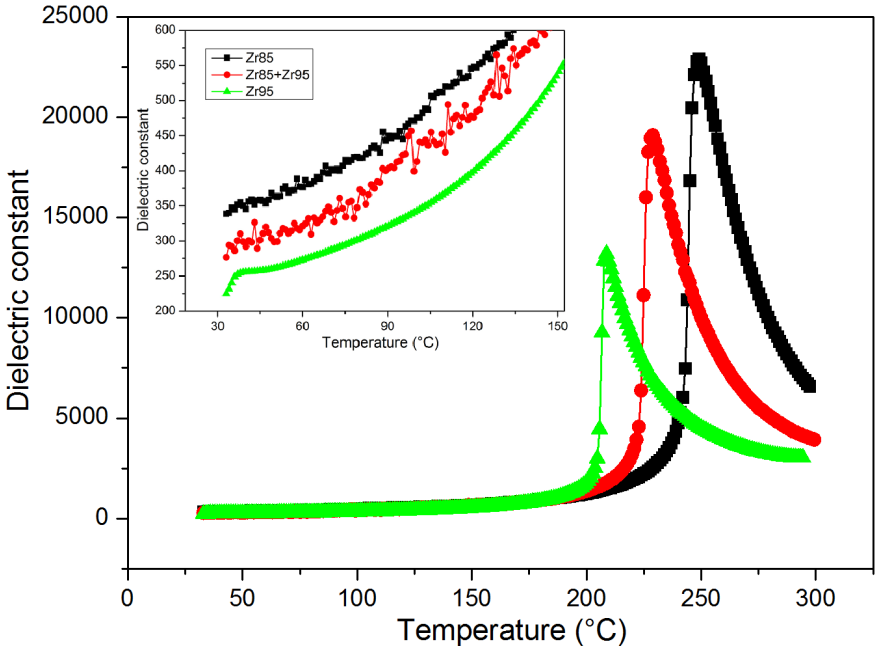

Fig.3. Temperature-dependent dielectric constant of the ceramics with various Zr content

heating. Clearly, all the ceramics with different compositions show only a single dielectric peak during the heating process, and no other phase transformation was observed. The dielectric constant in all the cases first increased gradually, and then decreased with increasing temperature. The dielectric peaks correspond to the phase transition from a ferroelectric to paraelectric phase and were observed at 250°C, 225°C and 214°C for Zr85, Zr85+Zr95 and Zr95, respectively, which correspond to the 'Curie temperature' (T_c). It can be seen in Fig.3 that as the Zr content increases in the ferroelectric ceramics, the T_c is shifted to lower temperatures and the peak value of the relative dielectric constant decreases. This is a result of the change in crystallographic structure with an increase in Zr content; as in Table 1. According to [19], the low temperature ferroelectric rhombohedral phase content of the ceramics had increased and the Curie temperature of rhombohedral is lower than that of tetragonal, i.e. the Curie temperature of $PbZrO_3$ (230°C) is lower than that of $PbTiO_3$ (490°C) [12]. Furthermore, the decrease of the Curie temperature affected the phase

temperature of the low temperature ferroelectric rhombohedral to the high temperature ferroelectric rhombohedral (F_{RL}-F_{RH}), which will be discussed later.

A small relative permittivity (ε) is advantageous for the application of ceramics in pyroelectric energy harvesting. Pyroelectric figure of merits (FOMs) have been adopted to evaluate the pyroelectric materials selection and design optimization problems and a high voltage responsivity can be expressed as $F_v = P/C_v \varepsilon\varepsilon_0$, where P, C_v, ε and ε_o are pyroelectric coefficient, voltage specific heat capacity, relative permittivity and permittivity of free space, respectively [1]. Here, C_v is defined as $C_v = \rho \cdot c_p$ where c_p and ρ are heat capacity and density, respectively and in the present work, C_v is considered as $2.5\times10^6 J/m^3K$ [6]. Generally, this pyroelectric FOM is used for material selection for energy harvesting and infrared sensors. In addition, thermal to electrical energy conversion is also an important application of pyroelectric materials. An energy harvesting FOM (F_e) is proposed, where $F_e = p^2/\varepsilon C_v^2$ [1, 5]. According to the aforementioned FOMs, a low relative permittivity is one requirement for greater performance of the pyroelectric voltage and thermal to electrical energy conversion for a given heat input.

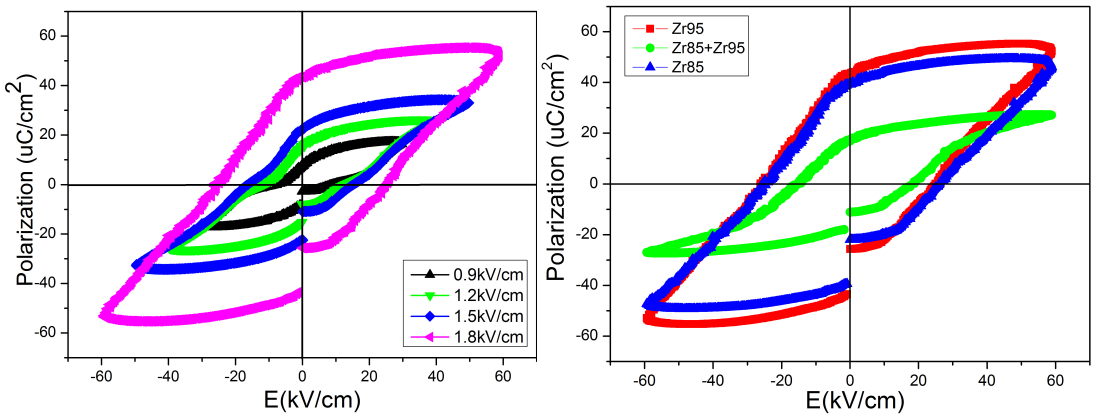

Fig.4. (a) Room-temperature polrisation – field (P-E) loops of the Zr95 ceramic at different electric field (b) the P-E loops of the Zr985, Zr85+Zr95 and Zr95 ceramics of various Zr content.

Fig.4. (a) shows the room-temperature P-E hysteresis loops of the Zr85, Zr95 and Zr85+Zr95 ceramics under different electric field at a meaurement frequency of 10Hz. As the electric field was increased, the remnant polarization (P_r) and the coercive field (E_c) increased, see Fig 4a. This can be explained that the higher electrical field can

lead to more domain switching along the direction of applied electrical field. As the electrical field is reduced, some domain are not aligned in the polarization orientation because of the crystallographic internal stress but when there the electrical field is removed, domain still remain in the orientation of polarization, termed the remanent polarization (P_r). Fig.4. (b) shows the P-E loops of the ceramics with various Zr content. Clearly, the P_r increased with increasing Zr content on comparing Zr95 with Zr85, and reached a maximum value of 43.3uC/cm^2 for Zr95 and 39.2 uC/cm^2 for Zr85. However, the P_r of Zr85+Zr95 decreased sharply to 17.0uC/cm^2. The crystallographic structure (relating to the Zr content) determines the ferroelectric properties of the ceramics and according to equation (3), we can use the saturated polarization P_S to evaluate the pyroelectric coefficients of the ceramics. When the coercive field is larger, the redirection of the spontaneous polarization becomes much harder, which is also likely to need a larger magnitude of temperature change. Thus, the higher remnant polarization and lower coercive field can be potentially beneficial to the greater performance of pyroelectric energy harvesting so that the polarization changes more rapidly with temperature [10].

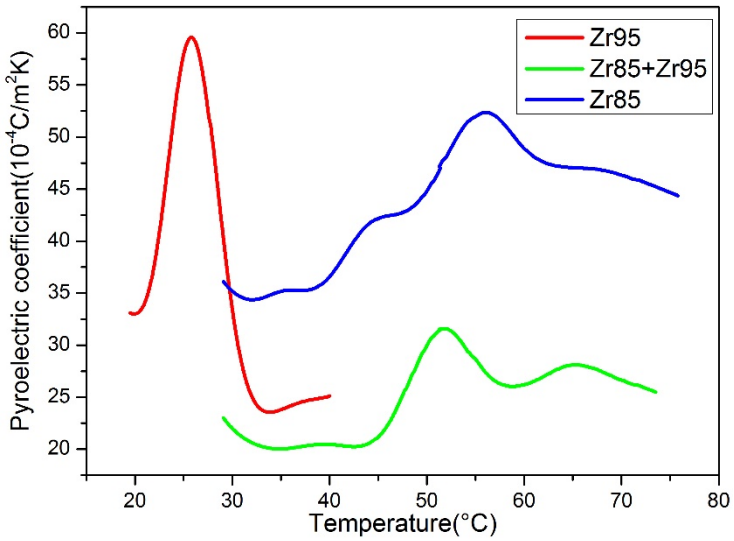

Fig.5. Pyroelectric coefficient as a function of temperature

The pyroelectric coefficients (p) of the ceramics with various Zr content are shown in Fig.5. As it can be seen in the figure, the pyroelectric coefficients of the ceramics increase with rise in temperature at first, becomes a maximum at temperature 25.8°C, 52.4°C and 57°C for Zr95, Zr85+Zr95 and Zr85, respectively, and decrease thereafter.

Clearly, the phase transition temperature of the F_{RL}-F_{RH} decreased with increasing the Zr content in the ceramics. The highest pyroelectric coefficient, $59.57\times10^{-4}C/cm^2K$ was obtained from the ceramic Zr95 at 25.8°C, which is almost two times as much as that of the ceramic Zr85+Zr95. Further, the temperature range of Zr95 is narrower than that of the other two ceramics. According to equation (3), the pyroelectric coefficient is closely related to the spontaneous polarization. At a phase transition, the spontaneous polarization induces nonlinear mutations, which release electric polarization energy and form a strong pyroelectric peak in a narrow temperature range [13]. This result is consistent with the aforementioned P-E loops.

The experimental and data processing of pyroelectric energy harvesting is shown in Fig.6. Temperature sensors were attached to the PMnN-PMS-PZT samples to monitor the temperature. The electrical output was measured with LabVIEW software connected to the voltage follower and data acquisition card. Fig.7. (a) shows the measured the cyclic change in temperature (from 18°C to 65°C) for all three ceramic systems. The rate change of temperature dT/dt were numerically calculated from measured data of temperature (T). The measured thermal fluctuations, dT/dt, and the corresponding generated voltage and current using a 10MΩ load resistance for Zr95, Zr85 and Zr85+Zr95 are shown in Fig.7. (b), (c), (d) and (e), respectively. The maximum value for voltage generated by the ceramic Zr95 with a sinusoidal thermal fluctuation, dT/dt, of 3.19°C/s peak was approximately 25.3V. According to the aforementioned equation (2), we can calculate the output power as shown in Fig.7(f). The maximum output power appeared in the ceramic Zr95 was 25.73uW. The results indicated that the ceramic Zr95 have a better pyroelectric energy performance than Zr85 and Zr85+Zr95, which was in good agreement with the above mentioned pyroelectric and ferroelectric properties.

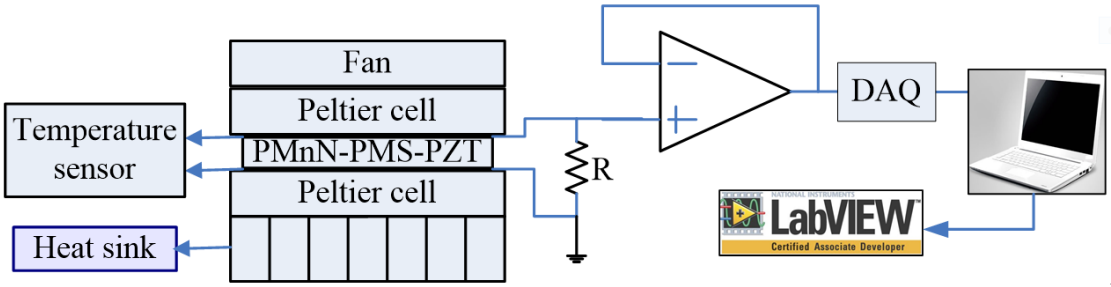

Fig. 6. Experimental and data processing schematic of the setup

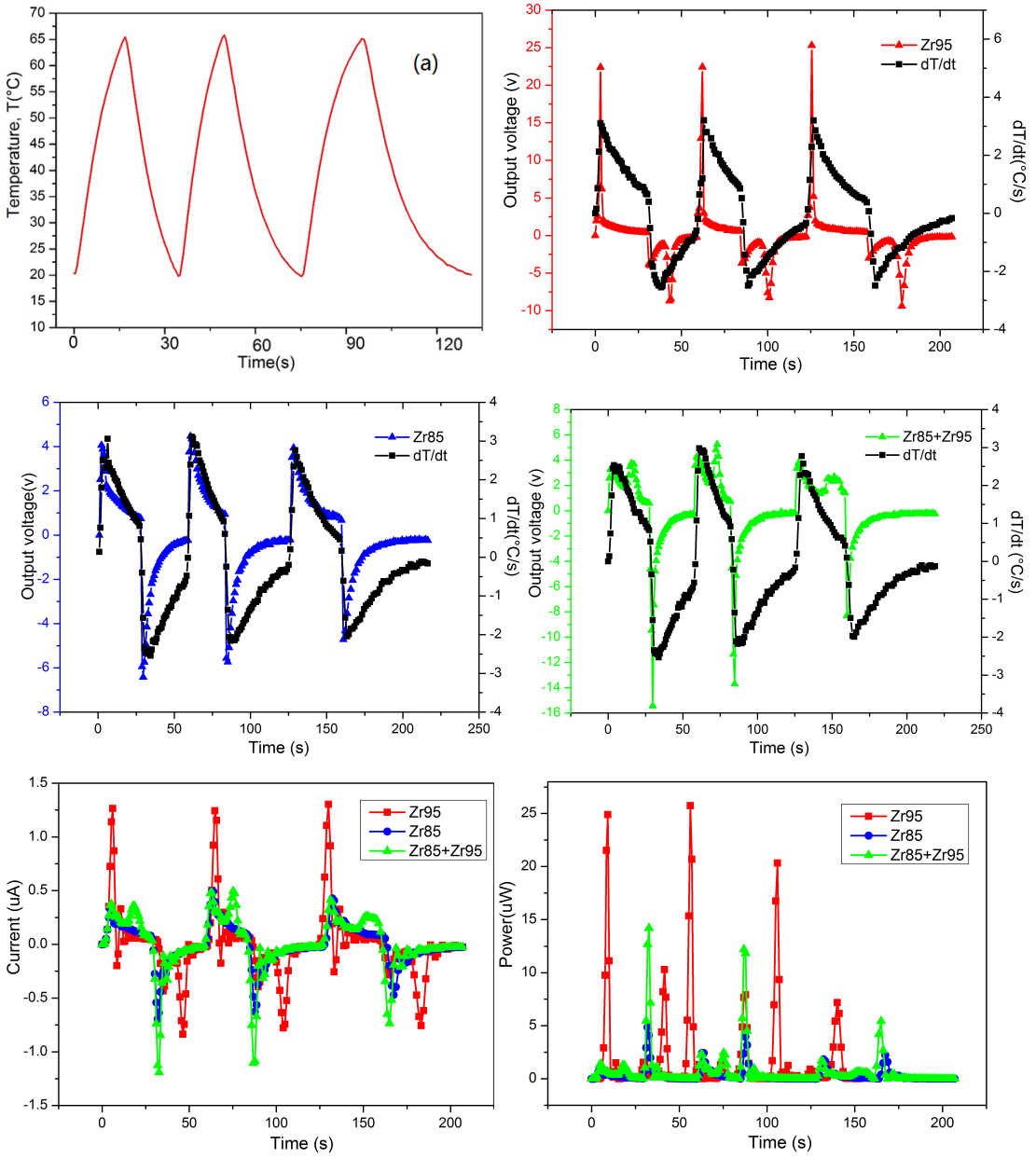

Fig.7. (a) The cyclic change in temperature and the output voltage and the rate change of temperature for Zr95(b), Zr85(c), Zr85+Zr95(d), respectively, (e) the current and (f) the output power.

4. Conclusions

The microstructure and electrical properties of PMnN-PMS-PZT ceramics with three different Zi/Ti compositions and the according application in pyroelectric energy harvesting performance was systematically discussed. With an increase in Zr content, the T_c shifted to lower temperatures and the peak value of the relative dielectric constant decreased which was a result of the change in crystallographic structure. The low temperature ferroelectric rhombohedral phase content of the ceramics had increased. The remanent polarization of Zr95 reached a maximum value of 43.3uC/cm^2. The maximum pyroelectric coefficient appeared in the ceramic Zr95 was 59.57×10^{-4} C/cm^{2}K at 25.8°C, which is almost two times as much as that of the ceramic Zr85+Zr95. With the use of Peltier cell and data acquisition card, the largest output current was obtained in the ceramic with Zr95 and the corresponding maximum output power was 25.73 uW, which indicate that the ceramic with Zr95 is a promising candidate for pyroelectric energy harvesting and the performance could be optimized by the proper phase structure control.

Acknowledgements

This work was supported by the innovation fund for the graduate students of Huazhong University of Science and Technology (Grant No. 0118650035).

References

[1] C.R. Bowen, J.Taylor, E.LeBoulbar, et al. Pyroelectric materials and devices for energy harvesting application. Energy. Environ. Sci., 7 (2014) 3836

[2] Zhonglin Wang. Triboelectric Nanogenerators as New Energy Technology for Self-Powered Systems and as Active Mechanical and Chemical Sensors. ACS Nano, 7 (2013) 9533

[3] Yan Zhang, Yinxiang Bao, Dou Zhang, and Chris R. Bowen. Porous PZT ceramics with aligned pore channels for energy harvesting applications. J. Am. Ceram. Soc., 98 (2015) 2980.

[4] B Hanrahan, L Sanchez, C M Waits and R G Polcawich. Improved pyroelectric

performance for thin film lead zirconate titanate (PZT) capacitors with IrO2 electrodes. Smart. Mater. Struct., 25 (2016) 015025.

[5] An-Shen Siao, Ching-Kong Chao and Chun-Ching Hsiao. Study on Pyroelectric Harvesters with Various Geometry. Sensors, 15 (2015) 19633.

[6] Ian M. McKinley, Felix Lee, Laurent Pilon. A novel thermomechanical energy conversion cycle. Appl. Energ., 126 (2014)78.

[7] Xiuyun Lei, Xianlin Dong, Chaoliang Mao, et al. Dielectric and enhanced pyroelectric properties of $(Pb_{0.325}Sr_{0.675})TiO_3$ ceramics under direct current bias field. Appl. Phys. Lett., 262901 (2012) 1.

[8] Shenglin Jiang, Pin Liu, Guangzu Zhang, et al. Enhanced pyroelectric properties of porous $Ba_{0.67}Sr_{0.33}TiO_3$ ceramics fabricated with carbon nanotubes. J. Alloy. Compound., 636 (2015) 93.

[9] He Fu-An, Lin Kai, Shi Dongliang, et al. Preparation of organosilicate/PVDF composites with enhanced piezoelectricity and pyroelectricity by stretching. Composites science and technology, 137 (2016) 138

[10] John A. Gallagher, Jian Tian, Christopher S. Lynch. Composition dependence of field induced phase transformations in $[0\ 1\ 1]_C$ PIN-PMN-PT relaxor ferroelectric single crystals with d_{322} piezoelectric mode. Acta Materialia, 81 (2014) 512.

[11] Abid Hussain, Nidhi Sinha, Sonia Bhandari, et at. Synthesis of 0.64 Pb(Mg1/3Nb2/3)O3-0.36PbTiO3 ceramic near morphotropic phase boundary for high performance piezoelectric ferroelectric and pyroelectric applications. J.Am.Ceram. Soc, 4 (2016) 337.

[12] Ting Yu, Guangzu Zhang, Yan Yu, et al. Pyroelectric energy harvesting devices based-on $Pb[(MnxNb_1\text{-}x)_{1/2}(MnxSb_1\text{-}x)_{1/2}]y(ZrzTi_1\text{-}z)_1\text{-}yO_3$ Ceramics, Sensor. Actuat. A-Phys., 223 (2015) 159.

[13] Deepakshi Sharma, Satyanarayan Patel, Anupinder Singh, Rahul Vaish. Thermal energy conversion and temperature-dependent dynamic hysteresis analysis for $Ba_{0.85}Ca_{0.15}Ti_{0.9\text{-}x}Fe_xZr_{0.1}O_3$ ceramics. J. Asian Ceram. Soc., 4 (2016) 102.

[14] D. Zabek, J. Taylor, V. Ayel, Y. Bertin, C. Romestant, and C. R. Bowen. A novel

pyroelectric generator utilizing naturally driven temperature fluctuations from oscillating heat pipes for waste heat recovery and thermal energy harvesting. J. Appl. Phys., 120 (2016) 1.

[15] Ning Duan, Carmen Arago & Julio A. Gonzalo. Ferroelectric Direct Energy Converters in Perspective. Ferroelectrics, 400 (2010) 321.

[16] Qingfeng Zhang, Maoyan Fan, Shenglin Jiang, et al. High pyroelectric response of low-temperature sintered $Pb_{0.87}Ba_{0.1}La_{0.02}(Zr_{0.7}Sn_{0.24}Ti_{0.06})O_3$ antiferroelectric ceramics. J. Alloy. Compound., 551(2013) 279.

[17] Hui Wei, Yongjun Chen. Synthesis and properties of $Pb(Zn_{1/3}Nb_{2/3})O_3$ modified Pb(Zr0.95Ti0.05)O3 pyroelectric ceramics. Ceram. Int., 40 (2014) 8637.

[18] W. Poprawski, Z. Gnutek, J. Radojewski, et al. Pyroelectric and dielectric energy conversion-A new view of the old problem. Appl. Therm. Eng., 90 (2015) 858.

[19] Guangliang Xie, Xiaotian Qu, Lijiang Zhang, et al. Fabrication and microstructure analysis of PZT. J. Test. Meas. Tech., 17 (2003) 278.